Adv. Space Res. Vol. 8, No. 9–10, pp. (9)447–(9)452 1988
Printed in Great Britain.

0273–1177/88 $0.00 + .50

PLASMA WAVES ASSOCIATED WITH DIFFUSE AURORAL ELECTRONS AT MID-ALTITUDES

J. R. Sharber,* J. D. Menietti,* H. K. Wong,* J. L. Burch,* D. A. Gurnett,** J. D. Winningham* and P. J. Tanskanen***

**Instrumentation and Space Research Division, Southwest Research Institute, San Antonio, TX 78284, U.S.A.*
***Department of Physics and Astronomy, University of Iowa, Iowa City, IA 52242, U.S.A.*
****Department of Physics, University of Oulu, SF 90570 Oulu 57, Finland*

ABSTRACT

Using simultaneous observations from the High Altitude Plasma Instrument and the Plasma Wave Instrument on board the Dynamics Explorer-1 satellite, we have examined 28 auroral zone crossings equally divided among dayside and nightside cases covering a range of Kp values from 1− to 8. We find that in the diffuse auroral region (CPS) electrostatic emissions of frequencies up to a few kHz are associated with low-energy, field aligned electron beams. Of 18 cases (11 nightside; 7 dayside) examined at high resolution in the particle data, 15 (9 nightside; 7 dayside) exhibited the field aligned beams with the electrostatic waves. In most cases the beams were upward-directed, but occasionally they traveled both up and down the field line. The three cases showing no beams occurred during intervals of Kp < 2. We interpret the electrostatic emissions as electron acoustic mode waves excited by the field aligned beams. A stability analysis based on the plasma parameters of one of the passes supports this interpretation.

INTRODUCTION

The most widely accepted model of the diffuse aurora involves the scattering by waves or turbulence of plasma sheet particles into the loss cone (e. g., see review by Ashour-Abdalla and Kennel /1/, and references therein). The particles undergo little acceleration before reaching the auroral ionosphere. Based on a report on OGO-5 observations /2/ showing strong wave emissions in the 1-10 mV/m range, Lyons /3/ developed a theory of diffuse auroral precipitation resulting from diffusion of electrons into the loss cone by electron cyclotron harmonic (ECH) waves. Using a bounce-averaged diffusion coefficient, he showed that the observed ECH waves would generally cause strong pitch angle diffusion of plasma sheet electrons of energies in the few tenths to few keV range. A later treatment of the problem /4/ that removed the bounce-averaging condition found that wave amplitudes required for strong diffusion of electrons were ~ 2.6 times greater than those computed by Lyons. The same paper showed that ECH waves observed by GEOS-2 were far less intense than the OGO-5 report had presented. Only 9% of the time did the waves exceed 2 mV/m, the amplitude required to put 1 keV electrons on strong diffusion. It thus appeared that the ECH waves, once thought to play a major role in diffuse aurora production, were not observed with sufficient intensity frequently enough to produce the required strong diffusion. More recent satellite studies /5, 6, 7, 8/ have given support to this conclusion. Thus it is clear that key questions regarding diffuse auroral particle precipitation still remain.

The launch of the Dynamics Explorer satellites in August 1981 provided the opportunity to study simultaneous measurements of plasma waves and auroral particles in the intermediate-altitude range. In the study, observations from the High Altitude Plasma Instrument (HAPI) /9/ and the Plasma Wave Instrument (PWI) /10/, both on DE-1, are examined in an effort to determine what relationships, if any, exist between the diffuse auroral particle population and the plasma waves. An earlier report using this data set /11/ showed that field-aligned electron beams are associated with wave emissions in the few hundred Hz to few kHz frequency range suggesting that the electron acoustic mode as the likely source of the emissions. In this paper we carry the analysis further by examining more of the passes at high resolution to confirm the presence of the beams and by including the results of a wave growth calculation using parameters obtained from the particle observations.

The study is based on a subset of DE-1 data consisting of 28 passes that range in altitude from 8000 to 22,000 km. Fourteen crossings were nightside cases; fourteen were dayside cases. They cover a wide range of magnetic activity with Kp varying between 1− and 8.

OBSERVATIONS

An example of the nightside observations is shown in Fig. 1. It occurred on day 296 (Oct. 23) of 1981 during the recovery phase of a storm. Kp was 4+ for the three-hour interval that included the pass. The spectrogram has three panels, the top of which is the downcoming (0° pitch angle) HAPI electron data. Auroral oval precipitation is seen between ~ 0341:20 UT (~ 67° IL) and 0351:30 UT (~ 60.1° IL). Within these latitudes the diffuse auroral region (or CPS) is seen between about 0349 UT (~ 62.2° IL) and 0351:30 UT (~ 60.1° IL). This lies within a region consisting mostly of downward field aligned current between 0348:40 and 0353:00 UT (J. Slavin, personal communication). The two lower panels are frequency-time spectrograms of the PWI electric and magnetic field amplitude measurements. In the auroral and polar regions are several types of emissions reported previously /12/. Electromagnetic emissions above the electron gyrofrequency (shown as the uppermost black dotted line on the data) are AKR /13, 14/. The emissions seen at latitudes down to 64.5° IL (0346 UT) are auroral hiss and are associated with the intense BPS particle precipitation /12/. Electromagnetic emissions seen at lower latitudes on the right end of the spectrogram are plasmaspheric hiss.

As shown in the figure, emissions associated with the diffuse auroral region are electrostatic in nature with frequencies up to a few thousand Hz. The two regions of greatest bandwidth and highest intensity appear to be associated with enhancements in the downcoming electron flux visible in top panel times near the 0349 and 0350 UT minute marks. On the spectrograms these appear as enhancements in the fluxes at low energies (i.e. ~ 20 eV to ~ 100 eV). They are visible immediately above the band of spacecraft-produced photoelectrons which have energies less than ~ 20 eV.

In order to look in detail at one of the regions of intense emission, we examine a high-resolution spectrogram, shown in Fig. 2(a). In this figure the top panel shows all HAPI electron data obtained from a single sensor between ~ 0348:50 and 0351:30 UT. The satellite spin is indicated by the pitch angle plot of the lower portion of the top panel. The second data panel shows PWI electric field data. In the HAPI spectrogram, highly collinated, field-aligned beams are seen at energies between ~ 20 and ~ 100 eV. In most cases the beams are upward directed, but in some cases they are counterstreaming. Attention is drawn on the figure to several such beams between ~ 0350 and 0350:30 UT. The contour plot of Fig. 2(b) is produced from a complete spin of DE-1 during the interval 0350:08–0350:14 UT. It clearly shows both the upward and downward directed beams visible in the spectrogram. A total of 11 passes have been analyzed in high resolution in the HAPI data. Beams of the kind shown in Fig. 2 were seen at diffuse auroral latitudes in 9 of these. It is possible that at times the beam energy is less than 20 eV. In such cases we would not detect it on DE-1 because of the spacecraft photoelectrons.

A pass characteristic of the dayside observations is shown in Fig. 3. It occurred on day 274 (Oct. 1) of 1981 during an interval characterized by a Kp of 2−. In this pass the boundary between the dayside diffuse auroral region and the cusp is located at 0741 UT (76.7° IL). The emissions in and poleward of the cusp at frequencies > 1 kHz are auroral hiss, a whistler mode emission investigated previously /12, 14/. Two types of emission are seen in the diffuse auroral region on this pass. One is the same emission present in the nightside observations having a frequency range up to a few kHz. This can be seen on the spectrogram at 0735:30 UT (75.8° IL). The high-resolution electron spectrogram (see inset above the normal spectrogram) shows the intense low-energy upgoing electron beams associated with these wave emissions. They are seen between ~ 0735 and ~ 0736 UT. For reference, a small pointer appears on each spectrogram panel at 0735:30 UT. Of seven dayside cases analyzed in high resolution in the particle data, six show electron beams of this kind. Combining the dayside and nightside results, the beams are present in 15 of 18 high-resolution spectrograms. The three cases where they were not observed are characterized by Kp < 2.

Another much more extended kind of emission is seen at diffuse auroral latitudes in Fig. 3. It is a relatively narrow band electromagnetic emission shown on the spectrogram between the lowest latitudes ~ 62.5° IL (at 0630 UT) up to at least 76.5° IL (at 0740 UT). It has a peak frequency of about 400 Hz, well below the electron gyrofrequency and a bandwidth of a few hundred Hz. Some of the signature shown in Fig. 3 may be plasmaspheric hiss /12/. However the emissions usually extend through latitudes spanning the entire CPS (diffuse auroral) region. On other passes there is sometimes a break between plasmaspheric hiss (which often peaks equatorward of the diffuse auroral equatorward edge) and a similar but usually lower frequency emission occurring well within diffuse auroral latitudes. We have identified this signature in all 14 of the dayside passes and in 9 of the 14 nightside cases analyzed. Based on these observations we have begun a separate study of this emission to be reported later.

DISCUSSION AND SUMMARY

The presence of the electron beams and their association with the enhancements in the broadband elec-

trostatic emissions suggests that the electron beams might be the source of the electrostatic waves. Since the observed electrostatic waves have a high frequency cutoff at a few kHz, which is less than the electron plasma frequency, the most probable candidates for these electrostatic waves are whistler waves or electron

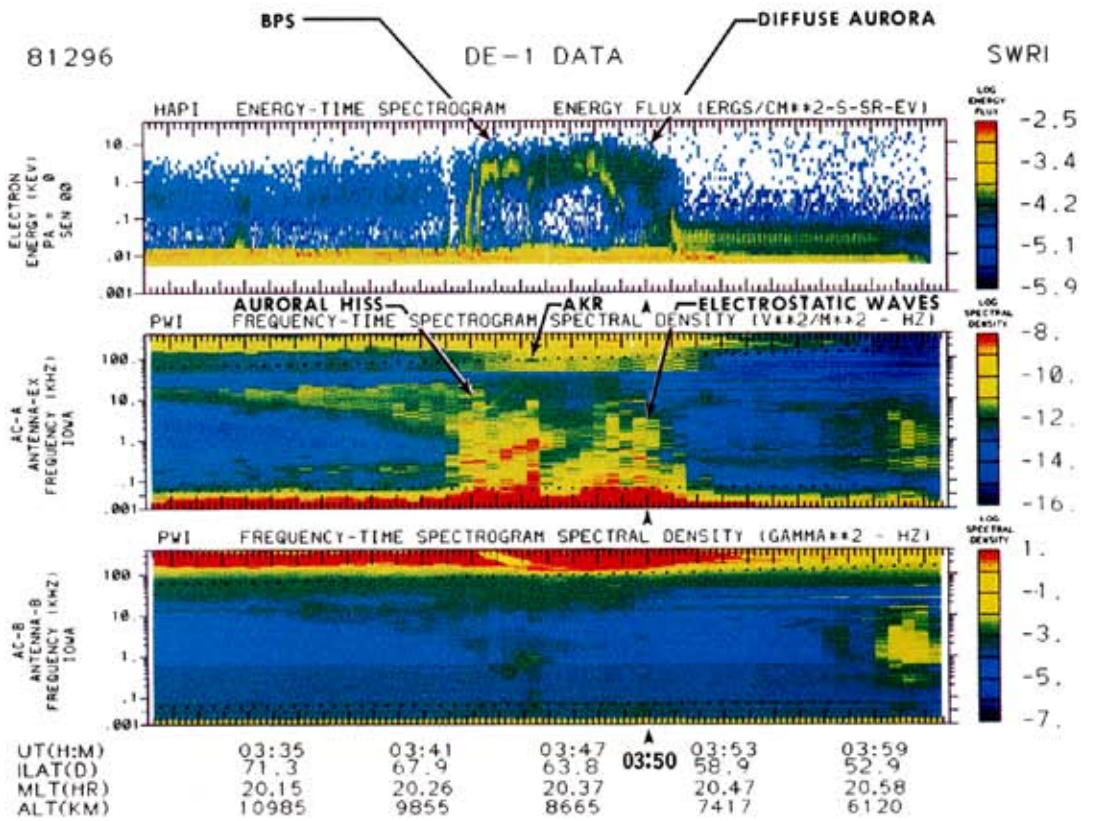

Fig. 1. Nightside example of simultaneous particle and wave measurements from DE-1 on day 296 (Oct. 23) 1981. HAPI measurements for 0° pitch angle electrons are shown in the top panel. The second and third panels are frequency-time spectrograms of the PWI electric and magnetic field amplitude measurements.

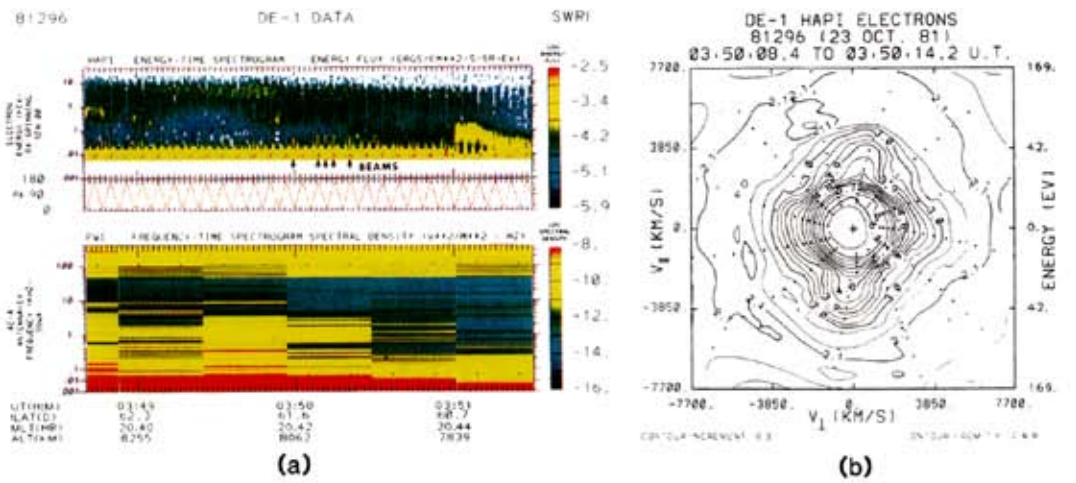

Fig. 2. (a) Expanded HAPI electron and PWI electric field spectrograms showing field aligned, low-energy electron beams. (b) Contour plot made from two spins of DE-1 between 0350:08 and 0350:14 UT.

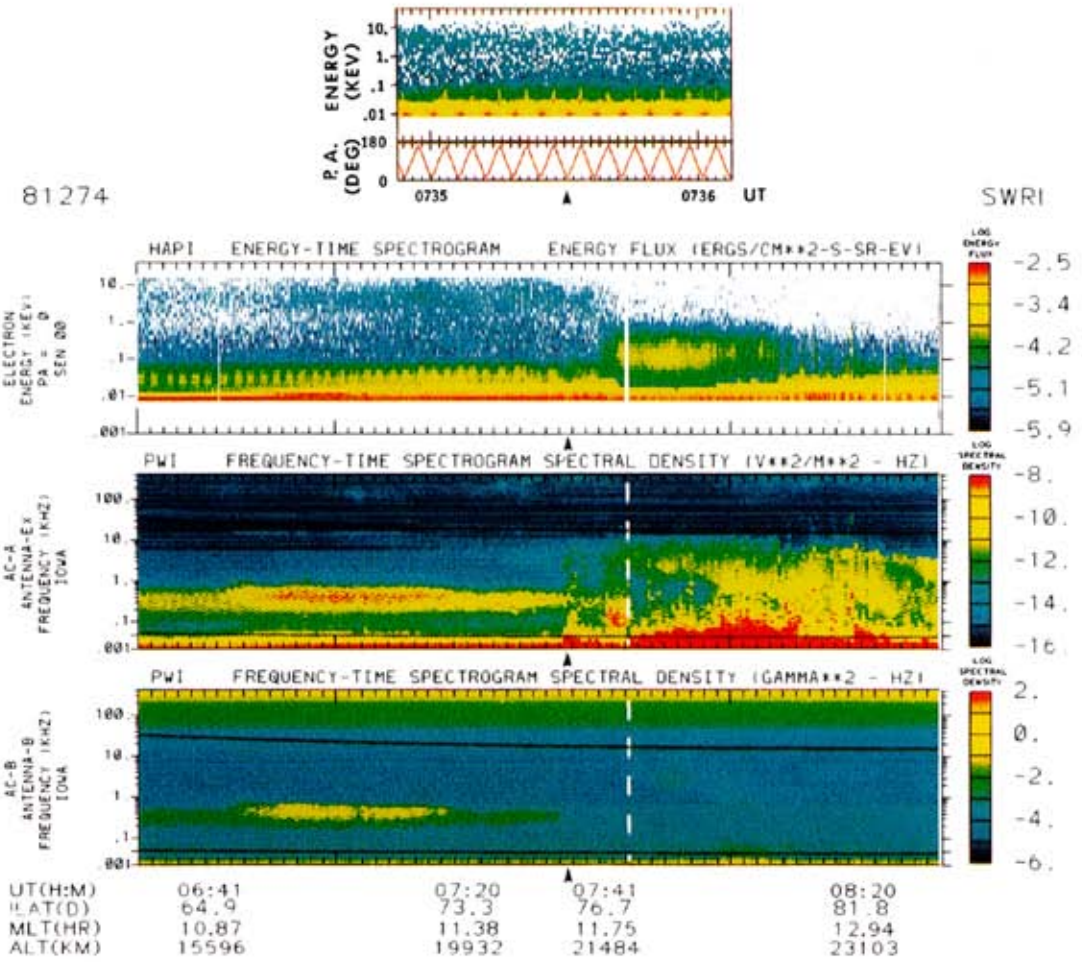

Fig. 3. Dayside example of particle and wave measurements. Beams are indicated in the expanded spectrogram inset at the top. For reference, a pointer on each panel marks the time at 0735:30 UT.

acoustic waves. The excitation of whistler and electron acoustic waves by electron beams in the polar regions has been thoroughly studied in the past few years /15, 16, 17, 18, 19/. One distinct feature of the beam-excited whistler waves is the funnel-shaped behavior in the frequency-time spectrogram /12/, which is not evident in our observations; thus, we speculate that these electrostatic emissions are generated in the electron acoustic mode.

In order to examine whether the electron beams can excite the electron acoustic waves in the observed frequency range, we have performed a stability analysis of the electron acoustic mode using the electron plasma parameters obtained between 03:50:08.71 and 03:50:08.91 UT of day 296 (see Figs. 1 and 2). During this sweep, the electron pitch angle varied from 171.2° to 173.9°. As determined from analysis of the HAPI electron data, the beam has a peak energy of 32 eV with a temperature of 8.6 eV, and a density of 2.32 cm^{-3}; the warm Maxwellian background electrons have a temperature of 46.1 eV and density of 0.73 cm^{-3}. Because of the spacecraft-produced photoelectrons, it is not possible to measure the density of the cold background electrons directly. We therefore perform our calculations by choosing three values of n_c (3 cm^{-3}, 2 cm^{-3}, and 0 cm^{-3}) and assuming a temperature of the cold electrons of 1 eV. The results are shown in Fig. 4 where the real and imaginary parts of the frequency are plotted as functions of the wavenumber. In the figure, the frequencies are normalized to the electron cyclotron frequency Ω_e, which has a value of 110 kHz at the time of the measurement; the wavenumber k is normalized to α_b/Ω_b (α is the beam thermal speed). As is clear from the figure, both the real frequency and the growth rate (ω_i/Ω_e) increase as the density of the cold electrons increases. This result is consistent with the results obtained by Lin *et al.* /17/ and is in agreement with the frequency range and broadband character of the emissions observed.

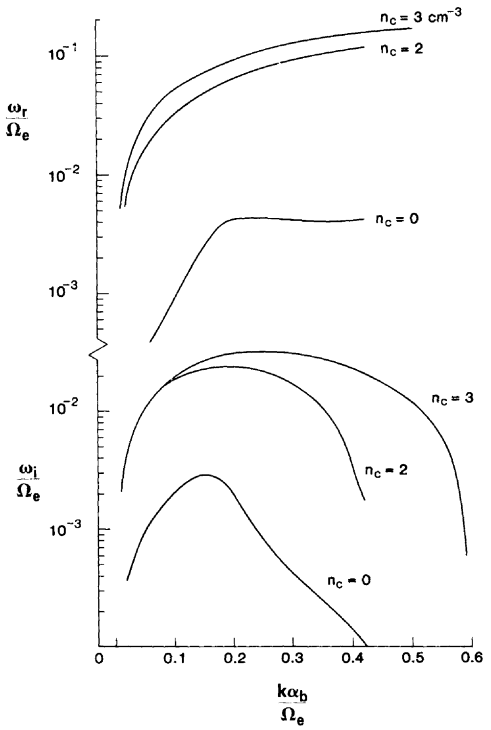

Fig. 4. Results of the stability analysis of the electron acoustic mode based on plasma parameters obtained from HAPI. Real and imaginary parts of the wave frequency are plotted vs. wavenumber for cold electron densities indicated on each curve. Real frequency and wave growth increase as the cold electron density increases.

In summary, we have examined 28 crossings of the auroral regions, equally divided among dayside and nightside cases, in which simultaneous measurements of particle and wave observations were made. We find that, in general, in the diffuse auroral regions, increases in intensity and bandwidth of electrostatic wave emissions are associated with low-energy, field-aligned electron beams. In particular, of 18 (11 nightside, 7 dayside) cases examined at high resolution in the particle data, 15 (9 nightside, 6 dayside) exhibited the field-aligned electron beams associated with electrostatic waves. In most cases the beams were upward directed, but in a few cases they were counterstreaming. The three cases in which no beams were seen took place within Kp < 2 intervals. We interpret the electrostatic emissions as electron acoustic mode waves excited by the beams. A growth rate calculation based on plasma parameters of one of the passes supports this interpretation.

ACKNOWLEDGEMENTS

The work was supported at Southwest Research Institute by AFOSR contract F49620–85–C–0029, NASA contracts NAS5–28711 and NAS5–28712, and NSF grant ATM–8713225. Work at the University of Iowa was supported by NASA/GSFC grant NAG5–310. We thank C. Lin for helpful discussions, J. Slavin for providing the magnetic field perturbations from DE-1, and R. Spinks and A. Ramirez for technical assistance.

REFERENCES

1. Ashour-Abdalla, M. and C. F. Kennel, Diffuse auroral precipitation, *J. Geomag. Geoelectr., 30*, 239, 1978.

2. Kennel, C. F., F. L. Scarf, R. W. Fredricks, J. G. McGehee and F. V. Coroniti, VLF electric field observations in the magnetosphere, *J. Geophys. Res., 75*, 6136, 1970.

3. Lyons, L. R., Electron diffusion driven by magnetospheric electrostatic waves, *J. Geophys. Res., 79*, 575, 1974.

4. Belmont, G., D. Fontaine and P. Canu, Are equational electron cyclotron waves responsible for diffuse auroral electron precipitation, *J. Geophys. Res., 88*, 9163, 1983.

5. Fairfield, D. H. and A. F. Viñas, The inner edge of the plasma sheet and the diffuse aurora, *J. Geophys. Res., 89*, 841, 1984.

6. Fontaine, D., S. Perraut, N. Cornilleau-Wehrlin, B. A. Paricio, J. M. Bosqued, D. Rodgers, Coordinated observations of electron energy spectra and electrostatic cyclotron waves during diffuse auroras, *Annales Geophysicae*, 86005A, 405, 1986.

7. Roeder, J. L. and H. C. Koons, A survey of electron cyclotron waves in the magnetosphere and the diffuse auroral electron precipitation, submitted for publication to *J. Geophys. Res.*, 1988.

8. Shumaker, T. L., M. S. Gussenhoven, D. A. Hardy and R. L. Corovillano, The relationship between diffuse auroral and plasma sheet electron distributions near local midnight, submitted for publication in *J. Geophys. Res.*, 1988.

9. Burch, J. L., J. D. Winningham, V. A. Blevins, N. Eaker and W. C. Gibson, High-altitude plasma instrument for Dynamics Explorer-A, *Space Sci. Instrum., 5*, 455, 1981.

10. Shawhan, S. D., D. A. Gurnett, D. L. Odem, R. A. Halliwell and C. G. Park, The plasma wave and quasi-static electric field instrument (PWI) for Dynamics Explorer-A, *Space Sci. Instrum., 5*, 535, 1981.

11. Menietti, J. D., J. R. Sharber, J. L. Burch and D. A. Gurnett, Plasma waves associated with electron beams in the diffuse auroral region, *Ionosphere-Magnetosphere-Solar Wind Coupling Processes, SPI Conference Proceedings and Reprint Series, 7*, Chang, Jasperse, Crew (eds.), Scientific Publishers, Cambridge, MA, 1988.

12. Gurnett, D. A., S. D. Shawhan and R. R. Shaw, Auroral hiss, Z mode radiation, and auroral kilometric radiation in the polar magnetosphere: DE-1 observations, *J. Geophys. Res., 88*, 329, 1983.

13. Gurnett, D. A., The earth as a radio source: Terrestrial kilometric radiation, *J. Geophys. Res., 79*, 4227, 1974.

14. Persoon, A. M., D. A. Gurnett and S. D. Shawhan, Polar cap electron densities from DE-1 plasma wave observations, *J. Geophys. Res., 88*, 10123, 1983.

15. Lin, C. S., J. L. Burch, S. D. Shawhan and D. A. Gurnett, Correlation of auroral hiss and upward electron beams near the polar cusp, *J. Geophys. Res., 89*, 925, 1984.

16. Tokar, R. L. and S. P. Gary, Electrostatic hiss and the beam driven electron acoustic instability in the dayside polar cusp, *Geophys. Res. Lett., 11*, 1180, 1984.

17. Lin, C. S., D. Winske and R. L. Tokar, Simulation of the acoustic instability in the polar cap, *J. Geophys. Res., 90*, 8269, 1985.

18. Roth, I. and M. K. Hudson, Simulations of electron beam excited modes in the high-altitude magnetosphere, *J. Geophys. Res., 91*, 8001, 1986.

19. Lin, C. S. and D. Winske, Simulation of the electron acoustic instability for a finite size electron beam system, *J. Geophys. Res., 92*, 7569, 1987.